Single-Frequency Linearly-Polarization Q-Switched Nanosecond Fiber Ring-Cavity Laser Enabled by an Electro-Optic Modulator

Siyu Chen, Dan Zhang, Wanru Zhang, Tao Wang, Can Li, Man Jiang, Jian Wu, Rongtao Su, and Yanxing Ma

***Abstract*—We report a single-frequency linearly-polarized nanosecond fiber ring-cavity laser based on an electro-optic modulator. A 0.08-nm-bandwidth fiber Bragg grating combined with a section of 1-m unpumped Yb-doped fiber act as an ultra-narrow bandwidth filter to realize single-frequency laser output. The devices used in the experiments are all polarization-maintaining to ensure the linearly-polarized laser output. Pulsed laser is obtained by using electro-optic modulator to adjust the loss in the laser cavity periodically. And the repetition rate of pulse trains can be flexibly changed from 550 to 1000 kHz with a pulse width of 27–59 ns. By varying the amplitude of the arbitrary function generator, we obtained a single-frequency pulsed laser output with a pulse width of 51–493 ns. The linewidth of the laser is 31.8 MHz, and the polarization extinction ratio was better than 20 dB.**

***Index Terms*—Single-frequency, pulsed laser, electro-optical modulator, linearly-polarized.**

I. Introduction

PULSED fiber lasers have garnered tremendous attention in recent years due to their applications like optical communications, materials processing, fiber sensing and spectroscopy [1], [2], [3], [4]. Fiber lasers have specific advantages compare to bulk optic counterparts related to their robust beam confinement, simple structure, easy integration, and environmental stability [5], [6]. In particular, pulsed fiber lasers operating in single frequency regime are more preferred in the fields such as lidar for the virtues of longer coherence length and narrower linewidth [7], [8], [9], [10], [11].

In general, the methods of pulse generation for single-frequency pulsed lasers include intensity modulation, gain switching and Q-switching. Intensity modulation is directly modulating the intensity of a continuous wave laser, which can produce pulsed laser with arbitrary repetition rate. Despite the merit of easily controllable pulsed parameters, this method suffers from considerable loss of the laser power. Thus, additional optical amplifiers are required for compensating the loss to meet the application requirements. Therefore, researchers have carried out relevant research on single-frequency pulsed fiber lasers based on gain-switching and Q-switching. The gain-switching operation, which modulates pump source, can periodically adjust the gain of the laser to achieve pulsed laser output. Researchers achieved single-frequency pulsed laser output at 1 μm and 2 μm by pumping a linear cavity with a pulsed laser source [12], [13], [14]. Q-switched operation of fiber lasers can be divided into passively and actively mechanism [15]. Passively Q-switched fiber lasers generally use passive complements such as semiconductor saturable absorber mirrors (SESAMs) or saturable absorbers (SAs) to realize pulsed laser output. Such lasers possess the advantages of user-friendliness, compactness, simplicity and flexibility of implementation [5]. In previous studies, stable single-frequency passive Q-switched laser was achieved at 1.5 μm and 2 μm by using SESAM in an ultrashort resonant cavity [16], [17], [18]. Li et al. added a two-dimensional material with saturated absorption characteristic into the resonator as the passively Q-switched element, and utilized an unpumped Er-doped fiber to realize the single-longitudinal-mode (SLM, which is the alternative name for single frequency) oscillation, thus achieved SLM pulsed laser output [19]. However, the repetition rate of the passive Q-switched pulse trains is difficult to fix, and it depends on the pump power in the laser cavity. It is almost impossible to change other parameters to adjust the repetition rate at a fixed pump power, which limits its application [20], [21]. Compared with passive Q-switching, active Q-switching possesses the advantages of producing laser pulses with narrower pulse width, higher peak power, well-controlled pulse repetition rate and stable performance [21], [22]. The common active Q-switched methods include the use of electro-optic modulator (EOM), acousto-optic modulator (AOM) and piezoelectric fiber stretcher (PZT stretcher). Researchers used PZT stretchers to change the loss in the cavity, combined with an ultra-short cavity or seed injection technique to obtain single-frequency pulsed laser [23], [24]. By modulating the loss of the laser cavity with an AOM, combined with seed injection technique, the researchers achieved single-frequency pulsed laser output

Manuscript received 30 March 2023; revised 22 May 2023; accepted 6 June 2023. Date of publication 9 June 2023; date of current version 16 June 2023. This work was supported in part by the National Natural Science Foundation of China under Grant 62275272 and in part by the Training Program for Excellent Young Innovators of Changsha under Grant KQ2206003. *(Corresponding author: Rongtao Su.)*

Siyu Chen, Wanru Zhang, and Tao Wang are with the College of Advanced Interdisciplinary Studies, National University of Defense Technology, Changsha 410073, China (e-mail: chensiyu21c@outlook.com; 1587977367@qq.com; wangtaobit@163.com).

Dan Zhang, Can Li, Man Jiang, Jian Wu, Rongtao Su, and Yanxing Ma are with the College of Advanced Interdisciplinary Studies, National University of Defense Technology, Changsha 410073, China, and with the Nanhu Laser Laboratory, National University of Defense Technology, Changsha 410073, China, and also with the Hunan Provincial Key Laboratory of High Energy Laser Technology, National University of Defense Technology, Changsha 410073, China (e-mail: smile203tt@163.com; lc0616@163.com; jiangman7@126.com; wujian15203@163.com; surongtao@126.com; xm_wisdom@163.com).

Digital Object Identifier 10.1109/JPHOT.2023.3284543

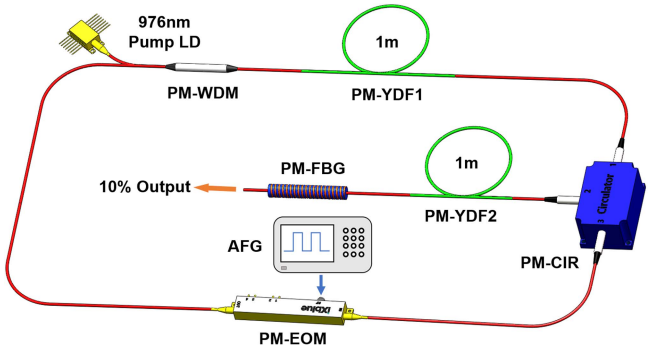

Fig. 1. Experimental setup of a single-frequency linearly-polarized nanosecond fiber ring-cavity laser.

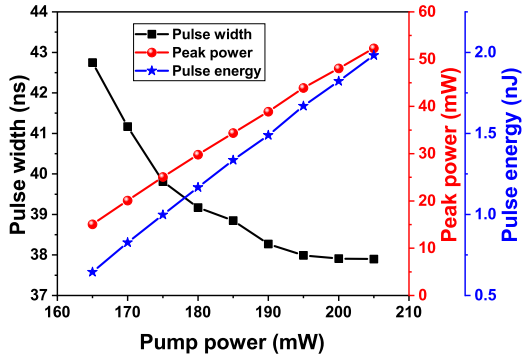

Fig. 2. Pulse width, peak power and pulse energy as a function of pump power at a repetition of 900 kHz.

at 1 μm and 1.5 μm [25], [26], [27]. Compared to the AOM, the EOM enjoys the advantage of shorter switch-time, which makes it more suitable for obtaining laser pulses with shorter pulse width [22]. Li et al. used an EOM as active Q-switching to achieve SLM pulsed laser output based on the injection seeding technique [28]. The pulse width of the above active Q-switching is alomost limited to the order of 100 ns and μs. The laser output with order of 10 ns is based on the seed injection technique, which will increase the complexity of the laser system by adding additional lasers. In addition, single-frequency pulsed fiber laser with linearly-polarized characteristic is more preferable for the virtues of higher detection sensitivity, higher combining efficiency and higher conversion efficiency. Consequently, a robust single-frequency pulsed fiber laser with linearly-polarized characteristic is demanded in terms of application and integration.

In this work, a single-frequency linearly-polarized nanosecond fiber ring-cavity laser enabled by an EOM is presented. An unpumped Yb-doped fiber together with a fiber Bragg grating acted as an ultra-narrow bandwidth filter to ensure single-frequency laser output. An EOM was used for modulating the loss of cavity to achieve pulsed laser output. Through parameter optimization, we finally realized stable single-frequency linearly-polarized nanosecond laser output with a central wavelength of 1064.6 nm, a pulse repetition rate of 550–1000 kHz, a pulse width of 27–493 ns, and a linewidth of 31.8 MHz.

II. Experimental Setup

The configuration of the single-frequency linearly-polarized nanosecond fiber ring-cavity laser is schematically shown in Fig. 1. The devices used in this experiment are all polarization-maintaining, and the connection between fibers is spliced by polarization maintaining fiber fusion splicer. As a result, this allows for an axis-to-axis connection between the fibers, thus ensuring the linear polarization operation in the system. The active fiber used in this experiment is a 1-m-long polarization-maintaining Yb-doped fiber (PM-YDF1), which has a core diameter of 6 μm and a cladding diameter of 125 μm. It was pumped by a 976 nm laser diode (LD) via a 976/1064 nm polarization-maintaining wavelength division multiplexer (PM-WDM). The laser system was forced to operate in the singe direction by a polarization-maintaining circulator (PM-CIR). A unpumped polarization-maintaining Yb-doped fiber (PM-YDF2) was used as a narrowband filter to realize SLM oscillation. The other end of the PM-YDF2 was connected by a polarization-maintaining fiber Bragg grating (PM-FBG). The central wavelength of the PM-FBG is about 1064 nm with a reflectivity of 90%, and the bandwidth is 0.08 nm. PM-FBG can preliminarily select longitudinal mode in resonator and extract 10% of the laser from cavity to output. A polarization-maintaining electro-optic modulator (PM-EOM) was applied for pulse generation. The PM-EOM (NIR-MX-LN-10-PD-P-P-FA-FA-20dB iXbule) is a $LiNbO_3$ intensity modulator based on Mach-Zehnder structure. The modulator has a modulation bandwidth of 10 GHz and a maximum DC bias voltage of 5 V. An arbitrary function generator (AFG) was used to apply modulated signals through the RF port of the PM-EOM.

A Fabry-Perot interferometer (FPI) and a photodetector (PD) were used to measure the frequency-domain and time-domain characteristics of the output laser. And the characteristics were recorded by a digital oscilloscope (DSO). The optical spectrum of the output laser was measured by an optical spectrum analyzer (OSA) with a resolution of 0.02 nm.

III. Results and Discussion

First, we investigated the influence of pump power on the pulse width, peak power and pulse energy. The AFG was set to a pulse wave with an amplitude of 2.4 Vpp, a duty-cycle of 26%, a rise and fall time of 5 ns, a bias voltage of 3.5 V, and a repetition rate of 900 kHz. We obtained single-frequency pulsed laser output at the pump power range of 165-205 mW, and the pulse width, peak power and pulse energy as a function of pump power are given in Fig. 2. In the Q-switched operation, an increase of the pump power at a fixed repetition rate could lead to a narrower pulse width. This phenomenon is associated with that a higher pump power provides a higher gain. And a higher gain leads to an increase of population inversion accumulated at the energy level. Therefore, the build-up time and extinguishing time of the pulse become shorter, so the pulse width gets shorter and the peak power becomes larger. As the pump power increases from 165 to 205 mW, the pulse width decreases from 43 to 38 ns. Meanwhile, the higher the pump power, the larger the pulse energy. The

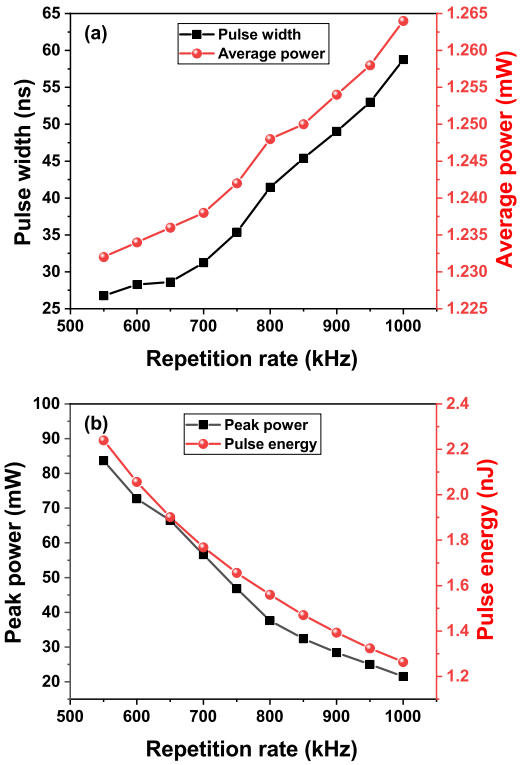

Fig. 3. (a) Measured pulse width and average power for the laser as a function of repetition rate under a pump power of 180 mW. (b) Calculated peak power and pulse energy of the laser as a function of repetition rate under a pump power of 180 mW.

maximum average power is 1.784 mW, corresponding to a peak power of 52.301 mW and a pulse energy of 2 nJ. When the pump power is lower than 165 mW, there is no signal light output due to the fact that the laser cannot oscillate for the pump power does not reach the threshold of the laser.

Then, we investigated the output characteristics of the pulsed laser at different repetition rates when the pump power was fixed at 180 mW. The AFG was set to a pulse wave with an amplitude of 2.4 Vpp, a duty-cycle of 26%, a rise and fall time of 5 ns and a bias voltage of 4 V. The single-frequency pulsed laser was obtained at repetition rate of 550–1000 kHz. The characteristics of laser pulse trains under a fixed pump power were measured, as shown in Fig. 3. As can be seen from Fig. 3(a), the pulse width gradually increases from 27 to 59 ns with increasing repetition rate. And under different repetition rates, the average power has a slight upward trend, but basically keeps around 1.24 mW. The pulse width increased with the increasing repetition rate because of the gain reduction on a single pulse [22]. The peak power and pulse energy decreased significantly as the increase of repetition rate, as plotted in Fig. 3(b). This is owing to that under the same pump power, increasing the repetition rate leads to a decrease in the energy-storing time. Therefore, the population inversion in the upper energy level does not have enough time to reach the maximum, thus the peak power of the output pulse will inevitably decline. At the same time, increasing the repetition rate leads to a larger number of pulses within a certain time, and the total energy remains unchanged at a fixed pump power.

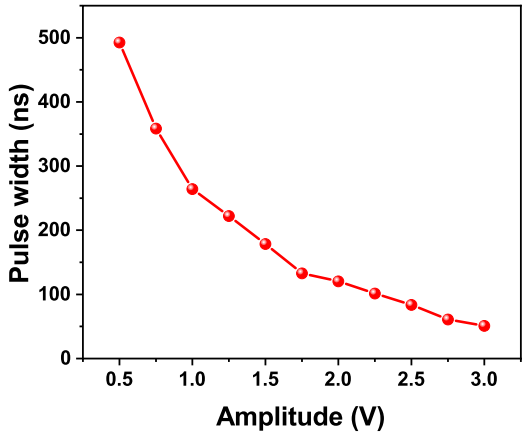

Fig. 4. Pulse width for the laser as a function of amplitude.

This leads to a decrease in the single-pulse energy. When the repetition rate was higher than 1000 kHz, the output pulse trains were unstable. This may be attributed to fact that increasing the repetition rate under a fixed pump power will lead to insufficient energy and low amplitude on a single pulse, thus unable to form stable pulse trains.

After that, the characteristics of laser pulses at different amplitude were investigated, as shown in Fig. 4. We set the AFG to a pulse wave with a duty-cycle of 26%, rise and fall times of 5 ns, the bias voltage of 5 V, and the repetition rate of 500 kHz. Meanwhile, the pump power was fixed at 160 mW. We obtained single-frequency pulsed laser output in the amplitude range of 0.5–3 Vpp. The pulse widths at different amplitudes are given in Fig. 4. As the amplitude increased from 0.5 to 3 Vpp, the pulse width decreased from 493 to 51 ns. In fact, adjusting the amplitude is to modulate the Q factor of the laser. The modulator used in the experiment is a $LiNbO_3$ electro-optic intensity modulator based on Mach-Zehnder structure. The input light is divided into two beams, and there will be a phase difference between these two beams of light in the process of transmission. The phase difference can be expressed as $\Delta\varphi = \pi V/V_\pi$, where V is the modulation voltage and V_π is the half-wave voltage. The intensity modulation is realized by the beam combining of two beams with phase difference. Therefore, by adjusting the amplitude of AFG, the modulation voltage can be changed. And the phase difference will be changed with the variation of modulation voltage, so as to adjust the loss in the cavity and realize Q-switched operation. By comparing the effects of pump power, repetition rate and amplitude on the pulse width, it can be seen that the amplitude has a much greater effect on the pulse width than the other two factors. Therefore, the pulse width of the output laser can be greatly reduced by increasing the amplitude.

To further the investigation of the pulse characteristics, we measured pulse trains and single-pulse envelop under different modulated waves, as shown in Fig. 5. First, we set the AFG to a pulse wave with a duty-cycle of 26%, rise and fall times of 5 ns, the bias voltage of 5 V, the amplitude of 2.5 Vpp, and the repetition rate of 600 kHz. Meanwhile, the pump power was fixed at 160 mW. Fig. 5(a) and (b) show the pulse trains and

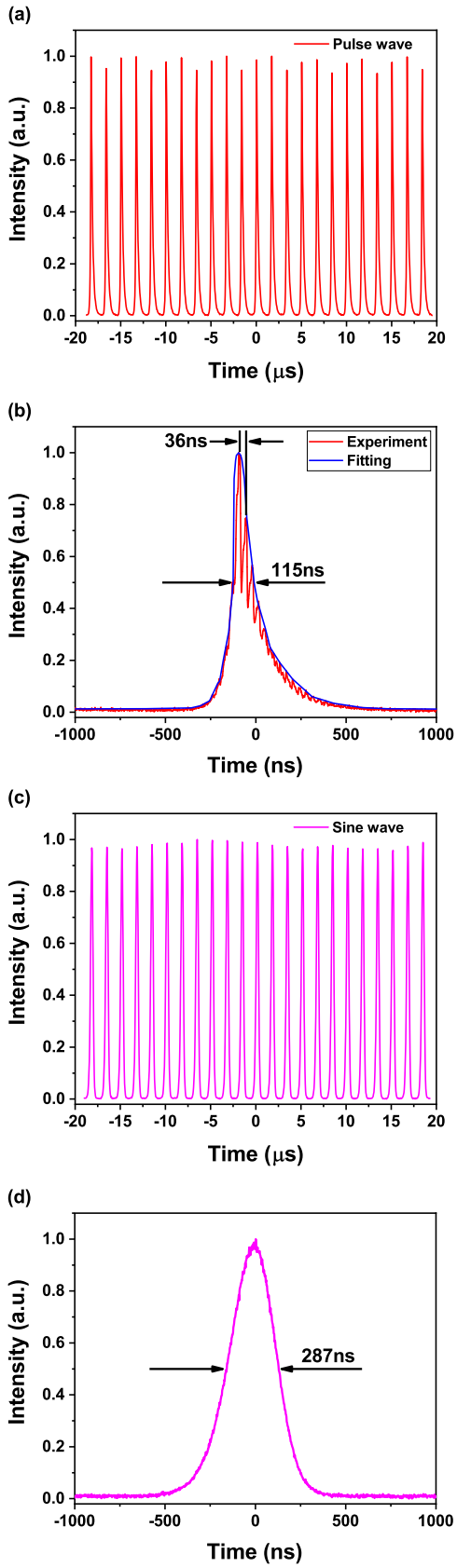

Fig. 5. (a) Pulse trains of the laser modulated by pulse wave. (b) Single-pulse envelop of the laser modulated by pulse wave. (c) Pulse trains of the laser modulated by sine wave. (d) Single-pulse envelop of the laser modulated by sine wave.

single-pulse envelope when modulated by pulse wave. It can be observed that there is multi-peak phenomenon in the output pulse. And it can be found that the time-difference between successive peaks in each pulse is approximately equals the photon roundtrip time, ∼36 ns (the cavity length is ∼10.3 m). The formation of multi-peak structure may be related to the short rise time of EOM when pulse wave is used for modulation. When the EOM is turned on, the broadband ASE is injected into the YDF via the EOM. And the rise time is only 5 ns, which is much smaller than the recovery time of the upper energy level particles of the YDF (∼μs [29]). Therefore, the injected broadband ASE induces the transient gain response of YDF, resulting in the initial ASE power fluctuations (initial transient peak) at the moment EOM is turned on. And the peak is gradually evolved into a multi-peak structure after several amplifications during the intracavity circulation [30], [31]. In order to verify the multi-peak structure is caused by the short rise time of EOM, we adopt the sine wave with longer rise time for modulation. Fig. 5(c) and (d) show the pulse trains and single-pulse envelope obtained by sine wave modulation. And the other parameters are the same as before. It can be seen that when sine wave modulation is adopted, no multi-peak structure is observed in the output pulse. It is further verified that the multi-peak structure of the pulse is caused by the short rise time of EOM when the pulse wave modulation is adopted.

The longitudinal mode characteristics of the laser were measured by a FPI, as shown in Fig. 6. The single-frequency performance of the laser is shown in Fig. 6(a). To achieve stable SLM operation, a 1-m-long unpumped PM-YDF2 is spliced with the 0.08-nm-bandwidth PM-FBG and serves as an ultra-narrow bandwidth filter. The PM-FBG will not only to enable laser to output but also help to form the SLM oscillation. It allows 10% of the laser output from the laser cavity, meanwhile it reflects 90% of the laser to the resonator. The reflected laser and the incident laser are two counter propagating waves, forming standing wave along the PM-YDF2 and induce spatial-hole-burning. Therefore, light intensity varies periodically along the PM-YDF2. And due to the saturated absorption characteristic, the light intensity will affect the refractive index of fiber. Consequently, the refractive index of the PM-YDF2 modulates periodically and results in a self-induced ultra-narrow bandwidth Bragg grating, which enables the single-frequency laser output.

However, when the peak power was too high, the laser changed from SLM regime to multi-longitudinal-mode (MLM) regime, as shown in Fig. 6(b). The high peak power can be result from the high pump power or the short pulse width, and the high peak power leads to the MLM oscillation. For example, we have obtained single-frequency pulsed laser at the pump power range of 165–205 mW under a fixed repetition rate of 900 kHz, as shown in previous discussion. With the pump power increasing to higher than 205 mW, the laser operated in the MLM regime. Similarly, as mentioned earlier, single-frequency pulsed laser was realized at the repetition rate range of 550–1000 kHz under a fixed pump power of 180 mW. When the repetition was below 550 kHz, the pulse width was so short that the peak power was too high, leading to the laser operated in the MLM regime. The MLM regime may be attributed to the fact that the dynamic grating is

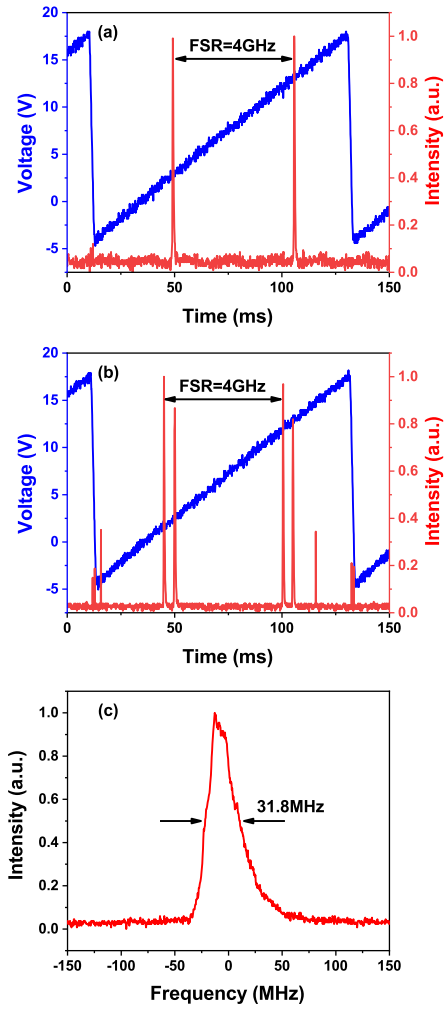

Fig. 6. (a) Single-frequency performance of the laser. (b) Multi-longitudinal-mode regime of the laser. (c) The linewidth of the laser.

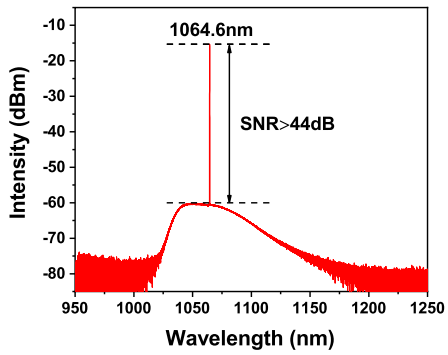

Fig. 7. Optical spectrum of the output laser within the measurement range of 300 nm.

destroyed under high peak power. A higher peak power will lead to a stronger grating owing to the increased modulation depth of the refractive index. And the stronger dynamic grating allows more light reflect back to the resonator, so less light is engaged in the formation of the grating, which will weaken the grating. As the weakening of the dynamic grating, the reflectivity decreases gradually. Consequently, the decreasing reflectivity will let more light pass the PM-YDF2 to take part in the formation of the dynamic grating, making a stronger grating again. At the higher peak power, it is a dynamic cyclical process and the characteristic of dynamic grating changes drastically all the time. It will significantly decrease the stability of dynamic grating and result in MLM oscillation [32]. The dynamic grating will be destroyed under high peak power, resulting in the inability to achieve single-frequency laser output. Consequently, the laser can only achieve single-frequency pulsed laser output at lower peak power, which will inevitably limit the peak power of the laser.

It takes enough time to build a dynamic grating for SLM selection based on a saturated absorber, and next we will discuss how to balance the stable SLM operation and pulse generation. As we know, the build-up and disappearance time of a dynamic grating built up from an unpumped doped fiber is determined by the excited-state lifetime of the doped ions [33]. This experiment was performed using ytterbium-doped fiber as a saturable absorber for single-frequency mode selection, and the excited-state lifetime of ytterbium ions is about ms level. Therefore, it is necessary to ensure that there is laser in the time range of ms level to participate in the formation of dynamic grating. However, the output laser of our experiment is pulsed laser, and there will be time that no laser output between one pulse and its adjacent pulse. And the time without laser output is related to the repetition rate, when the repetition rate is low enough, the time without laser output is long enough. When this time is comparable to the ms level, there is no laser involved in the establishment of dynamic grating during this time period, so the single-frequency mode selection mechanism cannot be established. Therefore, we can appropriately increase the repetition rate to ensure that there is laser in the time range of ms level to participate in the formation of dynamic grating, and finally realizes the SLM operation. In our experiment, the range of repetition rate is 550–1000 kHz, which corresponds to periods of μs level. That is, the time range without laser output is μs level, which is much smaller than the ms level required for SLM operation. Therefore, SLM operation and pulse formation can be realized simultaneously.

Fig. 6(c) gives the linewidth of the laser measured by FPI with a full width at half maxima (FWHM) of about 31.8 MHz. We also measured the polarization characteristics of the output laser by using an extinction ratio meter. The polarization extinction ratio (PER) of the output laser is greater than 20 dB at different pump powers, repetition rates and amplitudes.

Finally, the optical spectrum in the range from 950 to 1250 nm was recorded using an OSA with a resolution as high as 0.02 nm, as typically shown in Fig. 7. The central wavelength of the output laser is stabilized at 1064.6 nm with a FWHM linewidth as narrow as 31.8 MHz due to the single-frequency selection mechanism. The signal-to-noise ratio (SNR) was measured to be higher than 44 dB.

V. Conclusion

In conclusion, we have demonstrated a single-frequency linearly-polarized nanosecond fiber ring-cavity laser at 1064.6

nm. An EOM was used to initiate the active Q-switching to generate the pulse trains. An unpumped PM-YDF2 with saturated absorption characteristic was used as an ultra-narrow filter to realize stable single-frequency laser output. The laser was built with polarization-maintaining devices to achieve linearly-polarized laser output with a PER better than 20 dB. Finally, we realized single-frequency linearly-polarized pulsed laser output. The repetition rate could be continuously tuned from 550 to 1000 kHz, while the narrowest pulse is as short as 27 ns. By changing the amplitude of the modulation signal, we obtained the laser with pulse width of 51–493 ns. The linewidth of the laser is as narrow as 31.8 MHz and the maximum peak power of the output laser is 83.7 mW. The laser is supposed to be used as a seed source for master oscillator power amplifier to achieve a much higher peak power. After power amplification, the laser could be used in applications such as beam combining, coherent lidar, nonlinear frequency conversion, remote sensing and other fields.

References

[1] H. Hassan, M. A. Munshid, and A. Al-Janabi, "L-band dual wavelength passively Q-switched erbium-doped fiber laser based on tellurium oxide nanoparticle saturable absorber," *Laser Phys.*, vol. 30, no. 2, 2020, Art. no. 25101, doi: 10.1088/1555-6611/ab5a87.

[2] Y. Wang et al., "An all-optical, actively Q-switched fiber laser by an antimonene-based optical modulator," *Laser Photon. Rev.*, vol. 13, no. 4, 2019, Art. no. 1800313, doi: 10.1002/lpor.201800313.

[3] N. F. Zulkipli et al., "Generation of Q-switched and mode-locked pulses with Eu_2O_3 saturable absorber," *Opt. Laser Technol.*, vol. 127, 2020, Art. no. 106163, doi: 10.1016/j.optlastec.2020.106163.

[4] S. Liu, H. Huang, J. Lu, N. Xu, J. Qu, and Q. Wen, "Liquid-phase exfoliation of Ta_2NiS_5 and its application in near-infrared mode-locked fiber lasers with evanescent field interactions and passively Q-switched bulk laser," *Nanomaterials*, vol. 12, no. 4, 2022, Art. no. 695, doi: 10.3390/nano12040695.

[5] A. A. Shakaty, J. K. Hmood, B. R. Mahdi, R. I. Mahdi, and A. A. Al-Azzawi, "Q-switched erbium-doped fiber laser based on nanodiamond saturable absorber," *Opt. Laser Technol.*, vol. 146, 2022, Art. no. 107569, doi: 10.1016/j.optlastec.2021.107569.

[6] M. Xu, H. Chu, H. Pan, S. Zhao, and D. Li, "Highly stable passively Q-switched erbium-doped fiber laser with zeolitic imidazolate framework-67 saturable absorber," *Infrared Phys. Technol.*, vol. 125, 2022, Art. no. 104274, doi: 10.1016/j.infrared.2022.104274.

[7] R. Su, P. Zhou, X. Wang, H. Zhang, and X. Xu, "Active coherent beam combining of a five-element, 800 W nanosecond fiber amplifier array," *Opt. Lett.*, vol. 37, no. 19, pp. 3978–3980, Oct. 2012, doi: 10.1364/OL.37.003978.

[8] S. Fu et al., "Review of recent progress on single-frequency fiber lasers," *J. Opt. Soc. Amer. B*, vol. 34, no. 3, pp. A49–A62, 2017, doi: 10.1364/josab.34.000a49.

[9] Y. Chen, J. Zhang, X. Zhu, J. Liu, and W. Chen, "Development of pulse-profile-controllable 2-μm wavelength single-frequency all-fiber laser system operating at 10-Hz repetition rate," *Opt. Eng.*, vol. 58, no. 8, pp. 1–4, 2019, doi: 10.1117/1.Oe.58.8.086106.

[10] J. Wang et al., "High-power, high signal-to-noise ratio single-frequency 1 μm Brillouin all-fiber laser," *Opt. Exp.*, vol. 23, no. 22, 2015, Art. no. 28978, doi: 10.1364/oe.23.028978.

[11] K. Zhou, Q. Zhao, Z. Feng, C. Yang, and S. Xu, "An effective and universal intensity noise suppression technique for single-frequency fiber lasers at 1.5 μm," *Laser Phys.*, vol. 31, no. 7, 2021, Art. no. 075101, doi: 10.1088/1555-6611/abf5d2.

[12] R. Poozesh, K. Madanipour, and P. Parvin, "Single-frequency gain-switched ytterbium-doped fiber laser at 1017 nm based on dynamic self-induced grating in a saturable absorber," *Opt. Lett.*, vol. 44, no. 1, pp. 122–125, Jan. 2019, doi: 10.1364/OL.44.000122.

[13] W. Zhang et al., "Single-frequency linearly-polarized gain-switched DFB pulsed fiber laser," *Opt. Laser Technol.*, vol. 158, 2023, Art. no. 108808, doi: 10.1016/j.optlastec.2022.108808.

[14] S. Fang et al., "Gain-switched single-frequency DBR pulsed fiber laser at 2.0 μm," *IEEE Photon. Technol. Lett.*, vol. 34, no. 5, pp. 255–258, Mar. 2022, doi: 10.1109/lpt.2022.3149525.

[15] H. Ahmad, N. H. Mansor, S. A. Reduan, M. Z. Samion, N. Yusoff, and L. Bayang, "Passively high-power Q-switching in Er- and Er/Yb doped fiber with CdTe," *Opt. Laser Technol.*, vol. 156, Dec. 2022, Art. no. 108510, doi: 10.1016/j.optlastec.2022.108510.

[16] Y. Zhang et al., "Dual-wavelength passively q-switched single-frequency fiber laser," *Opt. Exp.*, vol. 24, no. 14, pp. 16149–16155, Jul. 2016, doi: 10.1364/OE.24.016149.

[17] Y. Zhang et al., "Compact passively Q-switched single-frequency Er^{3+}/Yb^{3+} codoped phosphate fiber laser," *Appl. Phys. Exp.*, vol. 10, no. 5, 2017, Art. no. 052502, doi: 10.7567/apex.10.052502.

[18] S. Fang et al., "Compact passively Q-switched single-frequency distributed Bragg reflector fiber laser at 2.0 μm," *Appl. Opt.*, vol. 60, no. 34, pp. 10684–10688, Dec. 2021, doi: 10.1364/AO.443962.

[19] W. Li et al., "212-kHz-linewidth, transform-limited pulses from a single-frequency Q-switched fiber laser based on a few-layer Bi_2Se_3 saturable absorber," *Photon. Res.*, vol. 6, no. 10, pp. C29–C35, 2018, doi: 10.1364/prj.6.000c29.

[20] Z. Yu, M. Malmstrom, O. Tarasenko, W. Margulis, and F. Laurell, "Actively Q-switched all-fiber laser with an electrically controlled microstructured fiber," *Opt. Exp.*, vol. 18, no. 11, pp. 11052–11057, May 2010, doi: 10.1364/OE.18.011052.

[21] Y. M. Peng et al., "Tunable and switchable multi-wavelength actively Q-switched fiber laser based on electro-optic modulator and an improved Sagnac filter," *Opt. Laser Technol.*, vol. 150, Jun. 2022, Art. no. 108001, doi: 10.1016/j.optlastec.2022.108001.

[22] Y. Shen et al., "200 μJ, 13 ns Er:ZBLAN mid-infrared fiber laser actively Q-switched by an electro-optic modulator," *Opt. Lett.*, vol. 46, no. 5, pp. 1141–1144, 2021, doi: 10.1364/ol.418950.

[23] Y. F. Zhang et al., "Compact frequency-modulation Q-switched single-frequency fiber laser at 1083 nm," *J. Opt.*, vol. 17, no. 12, 2015, Art. no. 125705, doi: 10.1088/2040-8978/17/12/125705.

[24] Q. Zhao et al., "Stable actively Q-switched single-frequency fiber laser at 1.5 μm based on self-injecting polarization modulation," *Opt. Exp.*, vol. 26, no. 13, pp. 17000–17008, 2018, doi: 10.1364/oe.26.017000.

[25] W. Li, H. Liu, J. Zhang, H. Long, S. Feng, and Q. Mao, "Q-switched fiber laser based on an acousto-optic modulator with injection seeding technique," *Appl. Opt.*, vol. 55, no. 17, pp. 4584–4588, Jun. 2016, doi: 10.1364/AO.55.004584.

[26] Y. Zhang et al., "Linearly frequency-modulated pulsed single-frequency fiber laser at 1083 nm," *Opt. Exp.*, vol. 24, no. 4, pp. 3162–3167, Feb. 2016, doi: 10.1364/OE.24.003162.

[27] W. Wang et al., "Seed-injected, actively Q-switched fiber ring laser using an AOM of zero-order transmission," *Opt. Commun.*, vol. 467, 2020, Art. no. 125747, doi: 10.1016/j.optcom.2020.125747.

[28] W. Li et al., "Mode-hopping-free single-longitudinal-mode actively Q-switched ring cavity fiber laser with an injection seeding technique," *IEEE Photon. J.*, vol. 9, no. 1, Feb. 2017, Art. no. 1500607, doi: 10.1109/jphot.2017.2654999.

[29] C. R. Giles, E. Desurvire, and J. R. Simpson, "Transient gain and cross talk in erbium-doped fiber amplifiers," *Opt. Lett.*, vol. 14, no. 16, pp. 880–882, Aug. 1989, doi: 10.1364/ol.14.000880.

[30] X. Lü, Q. Han, T. Liu, Y. Chen, and K. Ren, "Actively Q-switched erbium-doped fiber ring laser with a nanosecond ceramic optical switch," *Laser Phys.*, vol. 24, no. 11, 2014, Art. no. 115102, doi: 10.1088/1054-660x/24/11/115102.

[31] X. Chen, Q. Sun, J. Zhao, S. Feng, and Q. Mao, "Study on influences of amplified spontaneous emission on actively Q-switched ytterbium-doped fiber laser," *Chin. J. Lasers*, vol. 37, no. 8, pp. 1929–1933, 2010, doi: 10.3788/cjl20103708.1929.

[32] T. Yin, Y. Song, X. Jiang, F. Chen, and S. He, "400 mW narrow linewidth single-frequency fiber ring cavity laser in 2 um waveband," *Opt. Exp.*, vol. 27, no. 11, pp. 15794–15799, May 2019, doi: 10.1364/OE.27.015794.

[33] S. Zhao, "Research on multi-wavelength thulium-holmium co-doped fiber laser [D]," M.S. thesis, Dept. Opt. Eng., Huazhong Univ. Sci. Technol., Wuhan, China, 2014.